Heliyon 8 (2022) e12285

Contents lists available at ScienceDirect

Heliyon

journal homepage: www.cell.com/heliyon

Research article

Economic risk assessment of ammonium nitrate explosions at the Busan Port by determining the building damage using a 3D explosion simulation

Jae-Joon Lee [a], Tae-Yuun Ham [a], Woo-Song Jeong [a,b,*]

[a] Interdisciplinary Course for Crisis, Disaster and Risk Management, Sungkyunkwan University, Republic of Korea
[b] Republic of Korea Navy Lieutenant Commander, Republic of Korea

ARTICLE INFO

Keywords:
Hazards assessment
Vulnerability assessment
Economic risk
Risk assessment
Explosion impact analysis
3D explosion simulation
Building vulnerability
Ammonium nitrate
GIS
Chemical accident

ABSTRACT

Explosion-related disasters are large and difficult to predict; therefore, the magnitude of potential risks must be identified ahead of time. This paper presents a new method for evaluating economic risk based on building damage that can be carried out in advance. The study was conducted using scenario-based hazard analysis, vulnerability analysis, and risk assessment. Using the GIS (Geographic Information System) technique, spatial information of the damage target range was constructed, and the hazard analysis of the explosion accident was analyzed in connection with a three-dimensional explosion simulation. Vulnerability analysis based on impact was performed by reflecting building spatial information (location, material, and height), and economic risks caused by explosions in appropriate scenarios were confirmed by applying a new methodology that reflects the total area and building cost of 4708 building objects with an explosion radius of 3 km. The results revealed that the estimated damage costs of 44,616,934,076 won (~3.60000 US dollars) and 584,230,849,444 won (~476 million US dollars), respectively, provided the basis for policy decision-making for accident prevention. Using this study, the risk of explosion can be predicted in advance, and effective support for explosive storage buildings in terms of engineering, policy, and management is possible to minimize damage.

1. Introduction

This study aimed to advance engineering-based risk assessment technology, raise safety managers' awareness, and foster institutional development in the field of industrial safety. The reasons for conducting this study are based on the two categories of social importance. First, as the volume of goods shipped worldwide has increased, maritime traffic has also increased; a large number of explosive hazardous materials are stored at ports, and the size of each port is growing. Furthermore, as the volume of such goods increases, the risk of explosion has also increased. The majority of cargo volume is imported and exported by sea, and imported goods are stored in designated port storage facilities. Consequently, storage and management of cargo volume are critical. Second, as a safety blind spot develops for a large amount of hazardous material storage, safety managers' perceptions must change, and the role of an integrated control tower for the storage and management of explosive hazardous materials should be emphasized. The Korean Ministry of Oceans and Fisheries cannot currently monitor the handling of hazardous materials in real time under current legislation. Furthermore, the storage volume in the port can only be checked by the port operators, resulting in poor hazardous material management. In such social situations, policy measures such as disaster safety management and quantitative risk assessment are required to prevent explosion accidents, which are social disasters.

Three methods, namely, hazard analysis, vulnerability analysis, and risk assessment due to chemical explosions, were used in this study. We attempted to overcome the limitations of damage analysis during the hazard analysis stage. Previously, three-dimensional (3D) simulation required a considerable amount of time and effort owing to the design. Nonetheless, they allowed for the checking of hazard area and impact over a wide range using government-built building space information to evaluate the wide area efficiently and precisely As a result, it was possible to develop an evaluation method that could produce results in a short period when quick decisions were required. Hazard analysis was performed for an optimal scenario, and it was verified that 3D exposure simulation allowed for a more accurate hazard analysis. In the vulnerability analysis stage, the damage level according to the impact was reflected in the evaluation results. We attempted to reflect the materials of

* Corresponding author.
E-mail address: dnthd0319@naver.com (W.-S. Jeong).

https://doi.org/10.1016/j.heliyon.2022.e12285
Received 11 August 2022; Received in revised form 5 November 2022; Accepted 5 December 2022

the constructed building's spatial information because it was difficult to accurately evaluate the level of damage using only hazard analysis, which measures the intensity of damage. Previous studies measured strength by simulating an explosion or primarily investigated consequential approach; therefore, this study was aimed at determining a methodology that could reflect the degree of damage to a building by applying the concept of vulnerability. Finally, in the economic risk assessment stage, a method for economically converting the damage was used. By converting the degree of damage to economic value through a new attempt to consider the unit price and total floor area of the building, the manager can establish a disaster relief plan through intuitive judgment. Using the three innovative ideas and methods mentioned above, this study aimed to measure the quantitative economic risk at Busan Port, which has the highest cargo volume and load of the most hazardous materials in Korea. The findings of this study can be used as a reference for decision-making and protecting people's lives and property through decision-making support.

2. Literature review

Explosions of hazardous materials are constantly occurring worldwide. Ammonium nitrate is the most dangerous hazardous material, causing the most explosions. Ammonium nitrate is a commercially important substance, with more than 20 million tons consumed globally annually. Ammonium nitrate is primarily used in agricultural fertilizers and explosive materials around the world [1]. Several accidents still occur in the storage and transportation of ammonium nitrate, and there have been two recent major explosions in overseas ports, one in Tianjin, China, in 2015, and the other in Beirut, Lebanon. In 2020, several previous studies on the analysis of ammonium nitrate explosion accidents were conducted. These studies utilized methods that can be classified into three major categories: explosion accident analysis methods, safety management, and explosion risk assessments [2]. In [3], an explosion accident analysis method was used to confirm whether a large-scale explosion could be caused by a chemical reaction through explosion energy analysis of the explosion scenario. In [4], a scaling rule based on the crater diameter was used to estimate the amount of ammonium nitrate that had exploded. In [5], explosion safety management revealed that, when an explosive explodes, the structure that houses the explosive is over pressurized, resulting in a secondary explosion, which emphasizes the need to calculate safety distances, perform storage and safety management of ammonium nitrate, and ensure appropriate safety measures are in place. In [6], by analyzing the cases of ammonium nitrate explosion accidents, the importance of handling was emphasized by recognizing the risk of ammonium nitrate. In [7], the overloading of explosives material at ports was reported, and the authors emphasized that safety management should be strengthened through TNT equivalents. For large explosion accidents, consequence analysis and evaluation are primarily performed through investigations after their occurrence in the surrounding environment. Many researchers have conducted studies in diverse fields of explosion impact, hazard, vulnerability, and risk assessment to mitigate the damage due to such explosions. Consequently, diverse approaches are used to derive evaluation results, such as numerical simulation, on-site investigation, and statistical techniques, in small-and large-scale research. In previous studies related to explosion accident risk assessment, simulation-based analysis and various risk assessment methods were used. In [8, 9], the calculated level of damage caused by the pressure in an explosion was predicted based on the computational fluid dynamics (CFD) code of the vapor cloud explosion simulation. In [10], a safety assessment was conducted considering the work environment and employee health in explosion simulations. In [11], the coincidence rate between an actual explosion and a simulation based on the initial pressure and temperature of a boiling liquid expanding vapor explosion (BLEVE) was investigated. Hazard, risk, and vulnerability research has also been conducted to reduce damage and protect human lives. Furthermore, an explosion hazard assessment was conducted [12, 13] and evaluated [13] with the aim of protecting humans in the metal processing industry through the explosion hazard evaluation of magnesium–aluminum alloy powders. Moreover, in [12], the risk was estimated through a simulation of the process and mechanism of gas/coal dust explosions to improve the applicability of risk assessment results to prediction explosion impact. In [14], statistical techniques were used to perform a risk assessment based on gas explosions.

In [15, 16], a quantitative risk analysis was conducted and an assessment method was proposed to predict the explosion impact range. To prepare for the occurrence of a hazardous material explosion, Korea's Korea off-site risk assessment (KORA) quantitatively evaluates safety by taking into account the number of components, population density, and importance of surrounding buildings for the predicted impact range. As such, in previous studies, unlike those for earthquakes [17, 18, 19, 20, 21] and floods [22, 23, 24, 25], risk assessment methods for judging the explosion damage to buildings from an economical point of view and accurate spatial information have not been actively investigated.

3. Research flow chart

The study was conducted according to the flow chart in Figure 1 and was largely divided into two parts: an experimental setup for preparing the results and a risk assessment. In the first stage, we conducted a preliminary survey of the ExDAM 3D explosion simulation program and ammonium nitrate used in previous studies, constructed spatial information, and determined the explosion equivalent. In the second stage, we analyzed the physical risks (the level of damage according to the material of each object) through a simulation by analyzing the hazards and vulnerability. In this study, an economic loss calculation method using building usage information is presented for the conversion of the economic risk (R_E) caused by the physical risk (R_P) of an explosion at Busan Port.

4. Experiments

4.1. Materials

This study was conducted using both 3D explosion simulations and economic risk calculation processes. Geospatial and hazardous material information were used to implement a 3D explosion simulation for the same environment as that of the actual study area. Geospatial information comprises four types of data: orthogonal images, building locations, heights, and materials. Hazard material information consists of three types of data: material location (determines the explosion spot), storage capacity, and cargo volume. Damage and building asset values were used to calculate economic risk. The damage information data derived from the 3D explosion simulation included the damage ratio for 4708 buildings. The building asset value information consists of the standard unit price (cost for construction by unit) based on usage, total floor area, and building usage to ensure the loss of the study space. A description of the data and their sources is presented in Table 1.

4.1.1. Ammonium nitrate

According to the United States Environmental Protection Agency (EPA), ammonium nitrate is generally stable during use and unlikely to explode accidentally [26]. Despite being stable in air, it is a hazardous material that spontaneously explodes in the presence of oxygen accompanied by strong impact, friction, or exposure to high temperatures in a sealed state, such as a container [27, 28]. According to the Korea Fire Institute National Hazard Material Information System, ammonium nitrate is a first-class hazardous material and oxidative solid. The properties of ammonium nitrate are listed in Table 2 [1,6, 29–31].

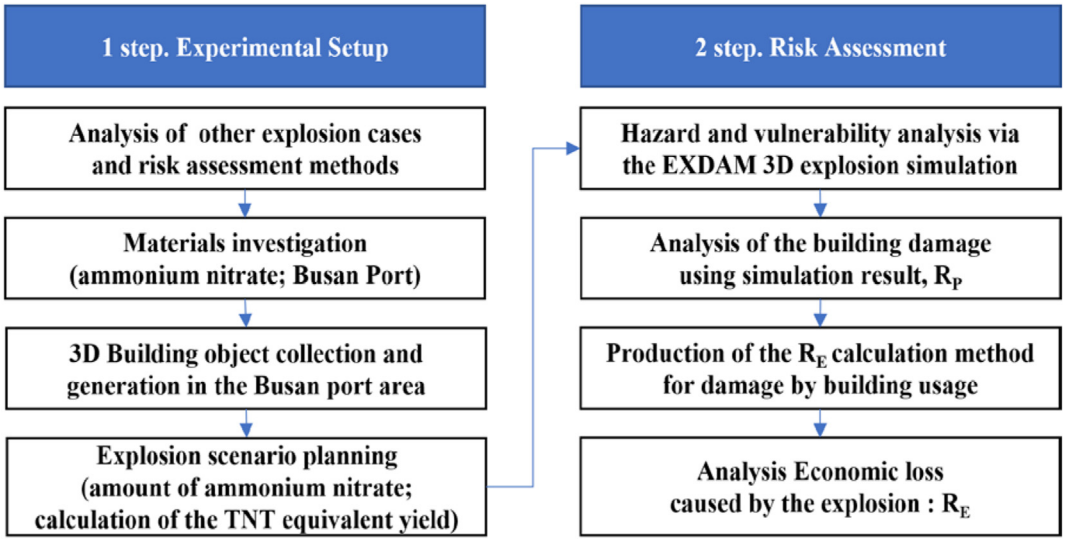

Figure 1. Research flow chart.

Table 1. Description and sources of the used data.

Division	List	Data	Description	Data source
3D explosion simulation	Geospatial information	Orthogonal mages	Used as a basic map for 3D simulations	MOLIT
		Building location	Used to assign an actual location in the 3D simulation to a building	NSDIP
		Building height	Used to calculate the shielding effect	NSDIP
		Material structure data	Used to reflect the vulnerability of the material structure data used to simulate the explosive impact	NSDIP
	Hazardous material information	Material location	Used to determine the explosion spot for hazardous material in the 3D simulation	MOF
		Storage capacity	Used to consider the actual storage capacity of hazardous material	MOF
		Cargo volume	Used to reflect the actual cargo volume	BROOF
Economic risk	Damage information	ExDAM output	Damage ratio for each of the 4708 structures used to calculate the cost of structure damage	ExDAM
	Building asset value information	Standard unit price based on building usage	Used to calculate the building asset by usage	REB
		Total floor area	Used to calculate the building asset by floor area	NSDIP
		Building usage	Used to distribute the building damage and asset	NSDIP

4.1.2. Study area: Busan Port

Busan Port is divided into new and northern ports. At the northern port, redevelopment projects are currently underway, and 22 berths of the new port (21 for containers and one for multipurpose) are currently operational. Furthermore, 34 berths are expected to be added to the NEW PORT by 2040, and it will become a designated megaton container and logistics hub port in Northeast Asia. Therefore, the number of imported, exported, and trans-shipment containers is increasing at the new port owing to the redevelopment of the northern port and an increase in container wharfs.

Table 2. Physical properties of ammonium nitrate.

Molecular weight	80 g/mol
Heat of combustion	346 cal/g
Heat of formation	1098 cal/g
Heat of explosion	346 cal/g
Heat of fusion	18.23 cal/g
Melting point	169.68 °C
Density	1.725 g/ cm^3

Busan Port handled 26,099 metric tons of ammonium nitrate in 2020, with imported and exported masses of 13,331 and 12,768 metric tons, respectively. According to the Hazardous Products Safety Control Act, ammonium nitrate should be stored and managed in outdoor storage facilities. Additionally, according to a 2020 MOF survey, most imported and exported ammonium nitrate is removed from the port within a week. As shown in Figure 2, the new port is divided into five wharfs, with one company operating each wharf. Therefore, loading and unloading ship operations are conducted at the wharf of each company, and hazardous materials are stored outdoors.

4.1.3. Geospatial information

Orthogonal images of suitable sizes were used to generate spatial data for the Busan New Port (Figure 3a). The building spatial data were generated using GIS general spatial information data, which are

Figure 2. Wharfs at the new Busan Port.

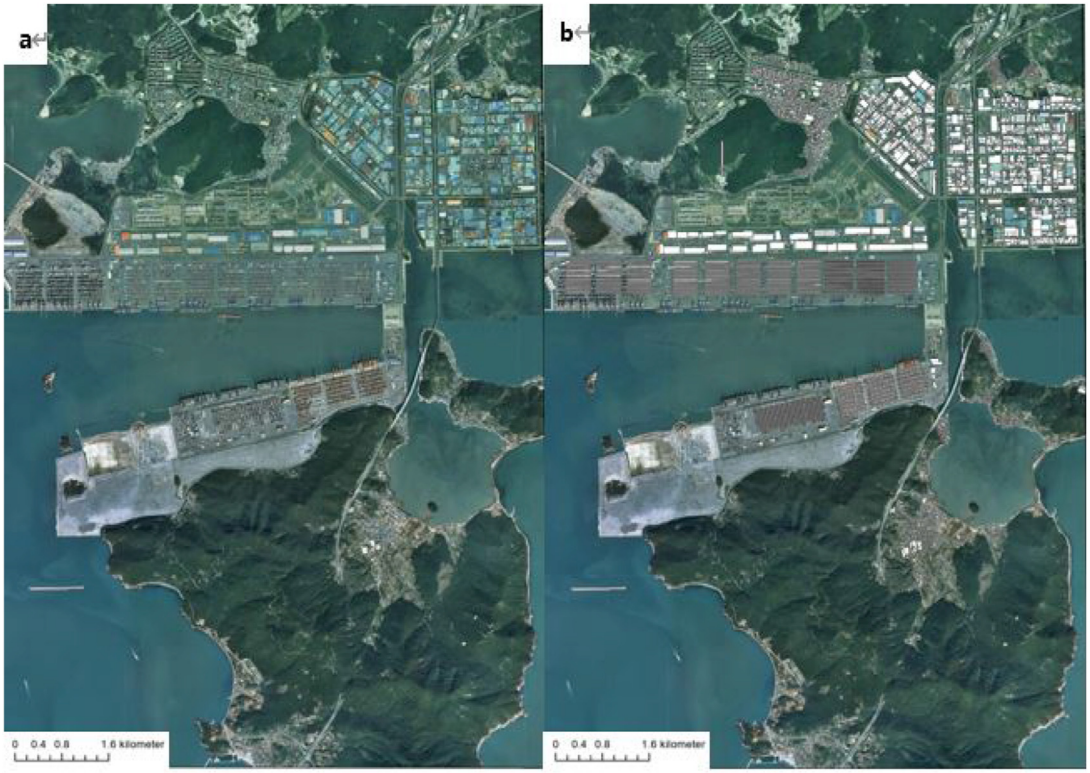

Figure 3. Generation of the spatial data: (a) map and (b) spatial data based on the map.

available on NSDIP's open application programming interface. Therefore, buildings not registered with government agencies were not included in the scope of data collection because of the difficulty in applying building standard unit prices. The generated spatial data yielded a dataset that combined comprehensive real estate data with the property data of a building ledger and included data on the location, usage, height, material, and building land area. These data were imported into ArcGIS, and the extracted data were used in the ExDAM 3D explosion simulation with set height values to yield 3D data (Figure 3b). For building data without a height value in the spatial data, the average height of the building type was determined by comparing satellite images. The material settings of the building were designated for each type using the property data, and containers for which data could not be retrieved from spatial data were generated based on the corresponding location in the orthogonal images. These containers were generated in accordance with the International Organization for Standardization regulations of 40 ft ($3.4 \times 3.4 \times 12$ m), which is most commonly used at sea. The scope of the simulation was set to a 3 km radius from Busan New Port, where hazardous materials are stored; and 4708 buildings with more than 20 usage characteristics, including detached houses, apartments, factories, and warehouse facilities. The structural material data of the building for the vulnerability analysis and the building usage data for the economic risk assessment are listed in Tables 3 and 4, respectively.

Table 3. Building structural material data for the vulnerability analysis.

Material Code	Building Structural Material Data	Building Number
M-1	003 Brick wall panel, 20 or 3 cm, non-reinforced	143
M-2	004 Concrete or cinderblock wall panels, non-reinforced	923
M-3	006 Steel (corrugated) paneling	7
M-4	007 Wood siding panels, standard house const.	349
M-5	018 Multi-story reinforced concrete frame office – non-eq.-res.	1362
M-6	019 Multistory reinforced concrete bldg. with concrete walls	1
M-7	021 Multistory steel-frame office, eq.-res. const.	19
M-8	022 Multistory steel-frame office, non-eq.-res. const.	1308
M-9	024 Lightweight steel building	596
Total		**4708**

bldg., building; eq., earthquake; res., resistant; const., construction.

4.1.4. Explosion scenario

In the scenario considered in this study, the amount of exploded ammonium nitrate was determined using two sets of data. The first dataset involved 2160 metric tons of ammonium nitrate stored at Busan Port according to the results of the 2020 BROOF survey. The second dataset involved 500.5 metric tons of ammonium nitrate, which is the 7-day stored average based on 26,099 metric tons of annual handling, according to the MOF. Of the five outdoor storage locations for hazardous materials at the five wharfs, the outdoor storage location of hazardous materials at the wharf closest to the residential building and logistics warehouse was set as the ammonium nitrate explosion site. This scenario was set as the worst case, based on evidence from past storage and cargo volume data. However, we did not consider the explosion of hazardous materials other than ammonium nitrate.

Table 4. Building usage data for the economic risk assessment.

Usage Code	Building Usage	Building Number
U-1	Apartments	3
U-2	Factories	1463
U-3	Educational Research and Welfare Facilities	15
U-4	Educational Research Facilities	18
U-5	Neighborhood Housing Facilities	46
U-6	Child and Geriatric Welfare Institutions	7
U-7	Detached Houses	2311
U-8	Animal- and Plant-Related Facilities	25
U-9	Cultural and Assembly Facilities	7
U-10	Business Facilities	13
U-11	Broadcasting and Communication Facilities	1
U-12	Hotel Facilities	13
U-13	Sports Facilities	2
U-14	Transportation Facilities	44
U-15	Medical Facilities	3
U-16	Recreational Facilities	1
U-17	Dangerous Article Storage and Disposal Properties	45
U-18	Automobile-Related Facilities	44
U-19	Residential Neighborhood Facilities/Class 1	128
U-20	Residential Neighborhood Facilities/Class 2	186
U-21	Religious Service Facilities	3
U-22	Storage Facilities	316
U-23	Shopping and Business Service Facilities	9
U-24	Shopping Service Facilities	5
Total		**4708**

5. Method

5.1. Concept of risk assessment

In this study, risk assessment was conducted to reduce the damage caused by potential explosions. Hazard and vulnerability are considered in the risk assessment process and are generally applied in various fields, such as in Eq. (1) [32, 33, 34, 35].

$$R(risk) = H(hazard) \times V(vulnerability) \tag{1}$$

where R (risk) refers to the probability of potential disaster losses (life, health status, livelihood, assets, and services) that may occur in society within a certain period, H (hazard) refers to the probability of a threat, and V (vulnerability) is the vulnerability characteristic of the elements at risk. In other studies [36, 37, 38, 39], V was calculated relative to A using Eq. (2), which represents the amount of consequence to the element at risk.

$$R = H \times V \times A \tag{2}$$

In this study, two scenarios based on the amount of ammonium nitrate stored outdoors at Busan Port were constructed to conduct a risk assessment. Here, H (hazard) refers to the explosion impact of stored ammonium nitrate, V (vulnerability) is the degree of damage to the structural material of the building under explosion pressure, and A is the cost of the building damage caused by the explosion. The risk was calculated as the total cost of building damage caused by explosives in an ammonium nitrate storage scenario.

5.2. TNT-equivalent yield

The effect of an explosion is generally determined by its intensity, which is calculated based on the TNT mass using the TNT-equivalent yield. The yield was used to analyze the damage-distance relationship with respect to the epicenter of an explosion by calculating the TNT-equivalent yields of various materials [40]. In addition, ExDAM requires a TNT-equivalent yield; therefore, we conducted a study to calculate the TNT-equivalent yield of ammonium nitrate. The methods for calculating TNT equivalents include pressure- and impulse-based [41] and Chapman–Jouguet [42] methods. Eq. (3), which is the TNT-equivalent conversion formula for explosion energy, is mainly used for the calculation.

$$W_{TNT} = \eta\left(\frac{\Delta H_c}{\Delta H_{TNT}}\right) W_G \tag{3}$$

W_{TNT} represents the mass of the TNT-equivalent, W_G is the mass of the explosive material, η is the efficiency factor for TNT, ΔH_c represents the heat of combustion of the explosive material, and ΔH_{TNT} represents the heat of combustion of the TNT.

Eq. (3) yields TNT-equivalent quantities based on the type of hazardous material, and the results differ according to the experimental environment, such as the experimental location, even when identical hazardous materials are used. Thus, the results will vary if the equations and environments used by researchers differ [43, 44, 45].

Studies of the TNT-equivalent yield of ammonium nitrate have been conducted in various fields. In a study comparing the power of explosives with that of TNT, the relative effectiveness factor (RE factor) of ammonium nitrate was 0.42 [7,46]. In another study on the risk due to the storage and transportation of ammonium nitrate in ports, the TNT-equivalent yield of ammonium nitrate was set to 0.346. Various values have been used in previous studies, generally ranging from approximately 0.3 to 0.55 [47].

In this study, we used 0.42, which is the value used by the United States Army [48] and the Korea Occupational Safety and Health Agency. This is expressed by Eq. (4): M_f represents the mass of ammonium nitrate,

M_{TNT} represents the TNT-equivalent mass, and the RE factor is the relative effectiveness factor of ammonium nitrate.

$$M_f(ton)\text{x}RE\ Factor(0.42) = M_{TNT}(ton) \tag{4}$$

5.3. Program tools: ArcGIS and ExDAM

This study used both the ArcGIS program (Esri, Redlands, CA, USA), a geographic information system (GIS) software used to generate spatial data for the Busan New Port, and the ExDAM 3D simulation program (Trinity Consultants, Dallas, TX, USA), which can model a complete 3D interactive explosion to simulate the explosion of ammonium nitrate. This program estimates the detailed building damage depending on material differences.

Using these two programs, we generated spatial data for Busan New Port and studied the risk of ammonium nitrate explosions. In this study, for the ExDAM 3D simulation program, the following data were analyzed: pressure calculations, pulse duration effects, shielding effects, and damage level [49].

5.3.1. Pressure calculations

The overpressure and dynamic pressure at a specified burst height and distance from the ground were determined by power decay interpolation between the two curves that bound the point [50]. As depicted in Figure 4, the pressure curves P_I and P_{I+1} are bound to point X, where the value of the pressure is desired. The distances R_I and R_{I+1} represent the slant ranges from ground zero (considering the height of the burst) to each of the pressure curves, measured along a line that passes through point X, and R represents the slant range from ground zero to point X. The pressure at any point is given by the interpolation equation [51]:

$$P = e^{C1}, \tag{5}$$

where

$$C1 = ln(P_I) - C2\ ln(R_I / R) \tag{6}$$

$$C2 = ln(P_{I+1} / P_I) / ln(R_{I+1} / R_I). \tag{7}$$

If a point falls outside the last pressure curve, it is extrapolated using the last two pressure-curve coefficients (C1 and C2).

5.3.2. Pulse duration effects

As the explosive yield increases, the corresponding pulse duration also increases. For a specified overpressure or dynamic pressure level, the longer the pulse duration, the greater the damage. For a fixed scaled distance $\left(\frac{distance}{yield}\right)^{1/3}$, the overpressure or dynamic pressure was essentially independent of the yield. However, because of the effect of pulse duration, the damage level remains dependent on the yield and increases as the yield increases. Structural materials classified as Q-type are more sensitive to this effect than P-type materials. For each structural material, two pulse duration factors (with values ranging from 0 to 10) were assigned, corresponding to moderate and severe damage, respectively. The pulse duration coefficient (K-factor) was used to correct for the pulse duration effect [52]. This method effectively uses the pulse duration factors K_m and K_S to adjust or correct (increase or decrease) the moderate and severe pressure levels P_m and P_S, respectively, thereby accounting for the increased or decreased pulse durations for a specified yield W relative to the structural material reference yield W_0.

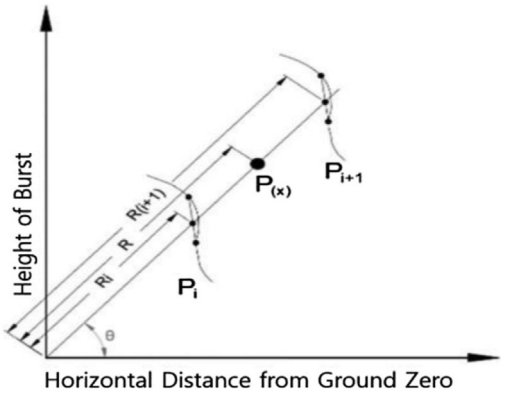

Figure 4. Graph for the pressure calculation method.

The adjusted pressure levels for P(Q)-type structures corresponding to moderate and severe damage, $P(Q)'_m$ and $P(Q)'_{s'}$ were corrected for this difference in the yield according to the following relation:

$$P(Q)'_i = P(Q)_i + \Delta P(Q)_i\ (i = m\ or\ s), \tag{8}$$

where

$$\Delta P(Q)_i = P(Q)_i\left(R_{P(Q)i} - 1\right), \tag{9}$$

$$R_{P(Q)i} = 1 - \frac{K_i}{10} + \left(\frac{K_i}{10}\right) R_{P(Q)i}^{\frac{1}{2}} \left(\frac{W_0}{W}\right)^{\frac{1}{3}}. \tag{10}$$

5.3.3. Shielding effects

For shielding effects, the direction of the blast wave must be considered relative to the orientation of the shielding structure block. The shielding effect of each structure indicates that the pressure differs depending on the shape of the structure, and the three directions (front, rear, or side) for each structure are interpreted with respect to the horizontal and vertical directions. This effect differs depending on the height relative to the length and width of the structure. To numerically interpret this effect, a shielding factor (S_F) was applied [53, 54].

$$S_F = \left(1 - V^2\right)^{\frac{1}{2}} \text{for } V^2 \le 1, \tag{11}$$

$$S_F = 0 \text{ for } V^2 > 1, \tag{12}$$

where

$$V^2 = \sum_{i=1}^{3} \left(\partial f_i / \partial x^*\right)^2 + \left(\partial f_i / \partial y^*\right)^2 + \left(\partial f_i / \partial z^*\right)^2. \tag{13}$$

If a shielding effect is present, structures that are not directly affected by this effect are inevitably affected. Subsequently, the shielding pressure of the structure was reduced, and the pressure reduction generated at this time, ΔP , is calculated using the following equation:

$$\Delta P = S_F P'_{12,} \tag{14}$$

where

$$P'_{12} = min(P_{1S'} P_2). \tag{15}$$

P_{1S} = pressure causing 100% damage or injury to shielding structure block.
P_2 = incident pressure (without shielding) in shielded structure block

The adjusted pressure, P'_2 at the shielded structure block is

$$P'_2 = P_2 - \Delta P. \tag{16}$$

5.3.4. Damage levels

The damage level relation for a "*P*" type structure/component is

$$d = d_m\left(P^{'}/P_m^{'}\right)^F, \tag{17}$$

where.

d = damage level.
$P^{'}$ = computed incident peak overpressure.

$$F = ln(d_m / d_s) / ln\left(P_m^{'} / P_s^{'}\right) \tag{18}$$

d_S = damage level threshold corresponding to severe damage or injury.
d_m = damage level threshold corresponding to moderate damage or injury.
$P_S^{'}$ = peak overpressure level causing severe damage to a p-type structure. Components corrected for pulse-duration effects
$P_m^{'}$ = peak overpressure level causing moderate damage to a P-type structure/component corrected for pulse duration effects.

The damage level relationship for a Q-type structure/component is

$$d = d_m\left(Q^{'}/Q_m^{'}\right)^G, \tag{19}$$

where.

d = damage level.
$Q^{'}$ = computed incident peak dynamic pressure.

$$G = 1.0 \text{ for } Q^{'} < Q_m^{'} \tag{20}$$

$$G = ln(d_m / d_s) / ln\left(Q_m^{'} / Q_s^{'}\right) \text{ for } Q^{'} > Q_m^{'} \tag{21}$$

$Q_S^{'}$ = peak dynamic pressure level causing severe damage to the Q-type structure/component corrected for pulse-duration effects
$Q_m^{'}$ = peak dynamic pressure level causing moderate damage to the Q-type structure/component corrected for pulse duration effects.

The moderate and severe damage level thresholds, d_m and d_S, are the percentage values of two of the three damage thresholds specified by the user at the model runtime [55].

Table 5. Average Standard unit price based on building usage.

Usage Code	Building Usage	Price (KRW/ m^2)
U-1	Apartment House	1 410 428
U-2, U-14	Factory	1 133 590
U-3, U-4	Educational Research Facilities	1 172 500
U-5, U-16, U-19, U-20	Neighbourhood Housing Facility	1 453 844
U-6	Child and Geriatric Welfare Institution	1 342 500
U-7	Detached House	1 640 448
U-8	Animal- and Plant-Related Facilities	652 667
U-9	Cultural and Assembly Facilities	1 591 833
U-10, U-11	Business Facilities	1 265 296
U-12	Hotel Facilities	1 497 782
U-13	Sports Facilities	1 513 625
U-15	Medical Facilities	1 643 667
U-17	Dangerous Article Storage and Disposal Properties	861 063
U-18	Automobile-Related Facilities	666 714
U-21	Religious Service Facilities	2 751 375
U-22	Storage Facility	989 456
U-23, U-24	Shopping Service Facilities	1 398 700

5.4. Calculating economic risk due to the explosions

In this study, we propose a new method to assess economic risk due to explosions, which is mainly used in the field of chemical disaster research using asset properties. The cost of building damage (refer to R_i) as a result of explosives is calculated using Eq. (22) by multiplying the building standard unit price (BAV in Eq. (23)) with the damage ratio obtained using the results of the ExDAM program.

In the case of the BAV, the total area (m^2) is obtained by summing the floor area of each floor of the building, including the basement, and multiplying it by the average standard unit price based on building usage, according to the REB (Table 5). The building usage applied to the BAV utilized GIS general spatial information data provided by the NSDIP. The NSDIP data are limited by the small number of city units that are not of the same usage, such as usage codes U-5, U-16, U-19, and U-20, but are sometimes classified differently. In this case, the deviation in the amount was the smallest, and similar usage was integrated. This method for calculating the BAV was used to calculate flood damage [56]. This method is also used to calculate the amount of damage caused by fire to determine the reconstruction cost of the lost area.

$$R_i = A(\mathrm{m}^2) \times P(\mathrm{KRW}/\mathrm{m}^2) \times D(\%) \tag{22}$$

$$BAV = A(\mathrm{m}^2) \times P(\mathrm{KRW}/\mathrm{m}^2) \tag{23}$$

R_i, A, P, and D represent the cost of building damage caused by explosives and the total floor area of the building, including the basement, average standard unit price based on building usage, and damage rate of the building, respectively, derived from the results of the ExDAM program.

6. Results and discussion

The results of this study were used to calculate the economic risk of possible future accidents. Existing studies on hazardous-chemical accidents deal with post-chemical accidents, as reported in [2] and [7]. The statistical analysis of chemical accidents in [57] is also based on past cases. In [58], risk analysis methods were proposed to determine the probability of future damage occurrence. In this study, human vulnerability studies were conducted on chemical leakage accidents and explosions using geospatial information [59]. In another study [60], 14 potential sources of direct economic impact were presented; however, damage to buildings was not considered. An analysis of the preceding chemical accidents revealed that research based on the economic risk of explosions to facilities and buildings is insufficient.

Therefore, this study confirmed R_E based on the amount of damage to a building from an economic perspective, in addition to simply checking the level of damage according to the material of the building. Figures 5, 6, 7, and 8 show the results of the simulation by classifying buildings by material. Figures 5 and 7 represent the damage areas identified through the simulation, and Figures 6 and 8 represent the damage (%), overpressure (kPa), and dynamic pressure (kPa) for each building object. The damage result (%) indicates the degree of damage to the building. The damage values were 5%, 30%, and 75% for slight, moderate, and severe damages, respectively. The damage values of the buildings are visually expressed by the colors in Figures 5 and 7. Figure 5 represents the results obtained by simulating the ammonium nitrate explosion are equivalent to 210.21 metric tons of trinitrotoluene: building damage. Figure 7 represents the results obtained by simulating the explosion of ammonium nitrate are equivalent to 907.2 metric tons of trinitrotoluene: building damage. The damage classification and levels are listed in Table 6 [49].

Therefore, the risk for each building object (R_i) was confirmed using Eq. (22) for the amount and damage (%) listed in Table 5. The result was derived as R_E in Eq. (24) by defining the total amount of damage expected for all building objects (n, total number of buildings in the study area):

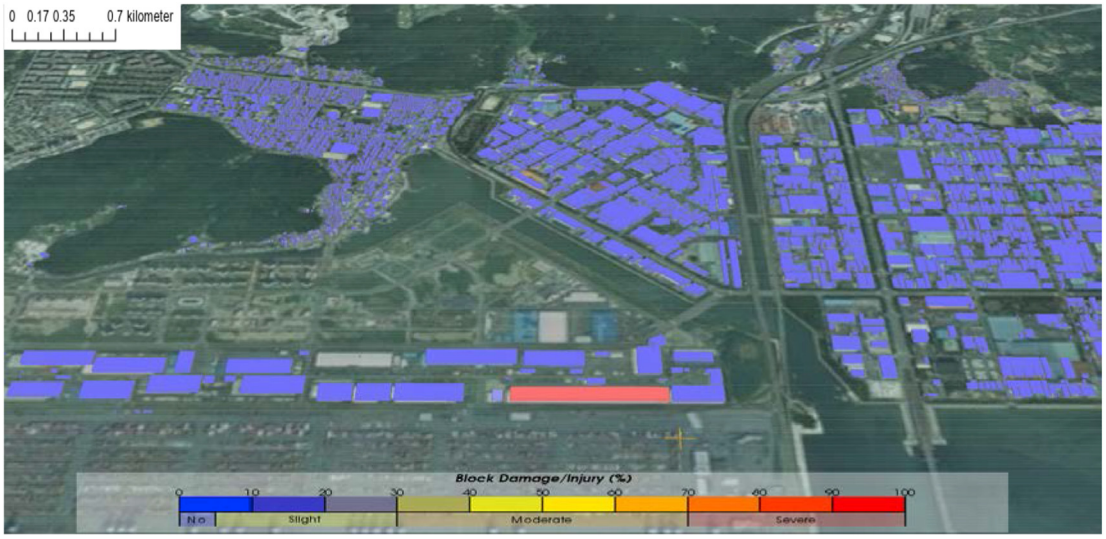

Figure 5. Results obtained by simulating the ammonium nitrate explosion equivalent to 210.21 metric tons of trinitrotoluene: building damage.

Structure	Structure			Structure	Structure		
	Damage (%)	Over Press. (kPa)	Dyn. Press. (kPa)		Damage (%)	Over Press. (kPa)	Dyn. Press. (kPa)
+☐ Kyungnam	15.0	6.78	0.16	+☐ Busan	100.0	68.4	15
++☐ Structure001(1)	0.0	1E-15	1E-15	++☐ Structure001(1)	8.5	3.45	0.0418
++☐ Structure002(1)	0.0	1E-15	1E-15	++☐ Structure002(1)	2.1	1.25	0.00546
++☐ Structure003(1)	0.0	1E-15	1E-15	++☐ Structure003(1)	0.0	1E-15	1E-15
++☐ Structure004(1)	0.0	1E-15	1E-15	++☐ Structure004(1)	0.0	1E-15	1E-15
++☐ Structure005(1)	0.0	1.46	0.00753	++☐ Structure005(1)	0.0	0.945	0.00314
++☐ Structure006(1)	0.1	2.03	0.0145	++☐ Structure006(1)	0.0	1E-15	1E-15
++☐ Structure007(1)	0.0	1E-15	1E-15	++☐ Structure007(1)	0.0	0.691	0.00168
++☐ Structure008(1)	0.0	0.277	0.00027	++☐ Structure008(1)	0.0	1E-15	1E-15
++☐ Structure009(1)	0.0	1E-15	1E-15	++☐ Structure009(1)	0.0	1E-15	1E-15
++☐ Structure010(1)	0.0	1E-15	1E-15	++☐ Structure010(1)	0.0	1E-15	1E-15
++☐ Structure011(1)	0.0	1.66	0.00963	++☐ Structure011(1)	0.0	3.22	0.0364
++☐ Structure012(1)	0.0	1E-15	1E-15	++☐ Structure012(1)	0.0	1.6	0.00905
++☐ Structure013(1)	0.0	0.239	0.000202	++☐ Structure013(1)	0.5	0.243	0.000209
++☐ Structure014(1)	0.0	1E-15	1E-15	++☐ Structure014(1)	0.0	1E-15	1E-15
++☐ Structure015(1)	0.0	1E-15	1E-15	++☐ Structure015(1)	4.9	0.647	0.00147
++☐ Structure016(1)	0.0	1E-15	1E-15	++☐ Structure016(1)	1.5	0.585	0.00121
++☐ Structure017(1)	0.0	0.713	0.00179	++☐ Structure017(1)	8.1	1.38	0.00671
++☐ Structure018(1)	0.0	0.444	0.000695	++☐ Structure018(1)	0.0	1E-15	1E-15
++☐ Structure019(1)	0.0	1E-15	1E-15	++☐ Structure019(1)	7.5	1.22	0.00527
++☐ Structure020(1)	0.0	1E-15	1E-15	++☐ Structure020(1)	0.0	1E-15	1E-15
++☐ Structure021(1)	0.0	0.182	0.000116	++☐ Structure021(1)	5.6	0.788	0.00218
++☐ Structure022(1)	0.0	1E-15	1E-15	++☐ Structure022(1)	0.0	1E-15	1E-15
++☐ Structure023(1)	0.0	1E-15	1E-15	++☐ Structure023(1)	0.0	1E-15	1E-15
++☐ Structure024(1)	0.0	1.03	0.00373	++☐ Structure024(1)	0.0	1E-15	1E-15
++☐ Structure025(1)	0.0	1E-15	1E-15	++☐ Structure025(1)	0.0	5.84	0.119

Figure 6. Tabular results of the ammonium nitrate equivalent to 210.21 metric tons of trinitrotoluene.

$$R_E = \sum_{i=1}^{n} R_i \tag{24}$$

Two scenarios were studied regarding the risk of explosions using the ExDAM program based on 500.5 or 2160 metric tons of ammonium nitrate at an outdoor storage location for wharf (1) at Busan New Port.

In the first scenario, an explosion was simulated based on 500.5 metric tons of ammonium nitrate. The calculated TNT equivalence was 210.21 metric tons. The building damage resulting from the ExDAM 3D explosion simulation is shown in Figure 5, Figure 6 shows the numerical results for the damage to buildings caused by the explosion. The results of the ammonium nitrate are equivalent to 210.21 metric tons of trinitrotoluene.

The 210.21 metric tons TNT-equivalent explosion affected 1352 of the 4708 buildings, with an estimated building damage of 44616934076 KRW (approximately 36,000,000 US dollars). The damage costs are listed in Table 7.

In the second scenario, an explosion was simulated based on 2160 metric tons of ammonium nitrate, which is equivalent to 907.2 metric

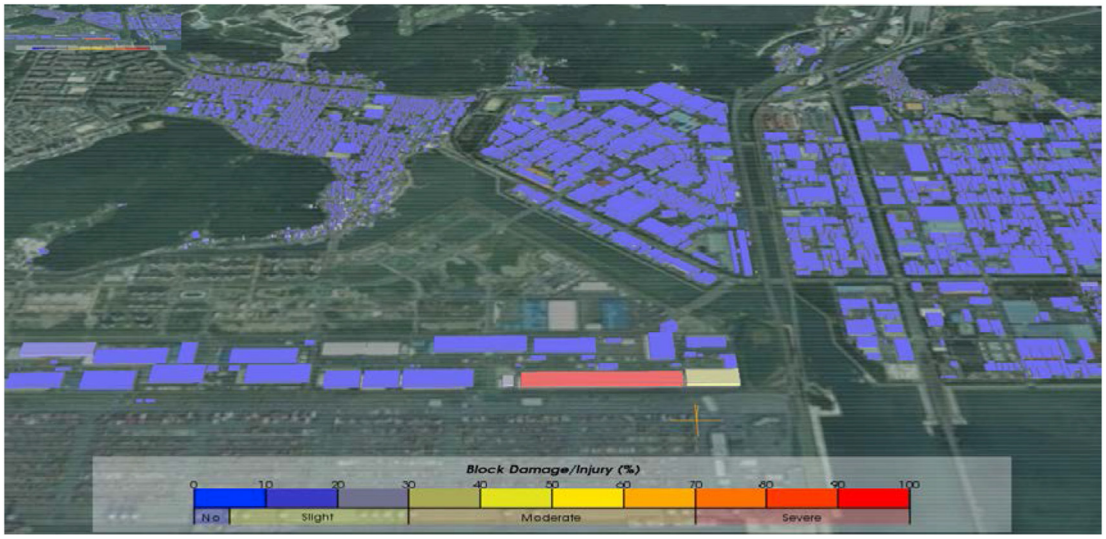

Figure 7. Results obtained by simulating the explosion of ammonium nitrate equivalent to 907.2 metric tons of trinitrotoluene: building damage.

Structure	Structure			Structure	Structure		
	Damage (%)	Over Press. (kPa)	Dyn. Press. (kPa)		Damage (%)	Over Press. (kPa)	Dyn. Press. (kPa)
+☐ Kyungnam	29.3	13.2	0.602	+☐ Busan	100.0	186	96.4
++☐ Structure001(1)	0.0	1E-15	1E-15	++☐ Structure001(1)	13.9	6.9	0.166
++☐ Structure002(1)	0.0	1E-15	1E-15	++☐ Structure002(1)	4.9	2.49	0.0217
++☐ Structure003(1)	0.0	1E-15	1E-15	++☐ Structure003(1)	0.0	1E-15	1E-15
++☐ Structure004(1)	0.0	1E-15	1E-15	++☐ Structure004(1)	0.0	1E-15	1E-15
++☐ Structure005(1)	0.1	2.93	0.0301	++☐ Structure005(1)	0.0	1.9	0.0126
++☐ Structure006(1)	0.1	4.06	0.0578	++☐ Structure006(1)	0.0	1E-15	1E-15
++☐ Structure007(1)	0.0	1E-15	1E-15	++☐ Structure007(1)	0.0	1.35	0.00637
++☐ Structure008(1)	0.0	0.554	0.00108	++☐ Structure008(1)	0.0	1E-15	1E-15
++☐ Structure009(1)	0.0	1E-15	1E-15	++☐ Structure009(1)	0.0	1E-15	1E-15
++☐ Structure010(1)	0.0	1E-15	1E-15	++☐ Structure010(1)	0.0	1E-15	1E-15
++☐ Structure011(1)	0.1	3.31	0.0385	++☐ Structure011(1)	0.1	6.47	0.146
++☐ Structure012(1)	0.0	1E-15	1E-15	++☐ Structure012(1)	0.0	3.22	0.0364
++☐ Structure013(1)	0.0	0.479	0.000806	++☐ Structure013(1)	1.2	0.488	0.000837
++☐ Structure014(1)	0.0	1E-15	1E-15	++☐ Structure014(1)	0.0	1E-15	1E-15
++☐ Structure015(1)	0.0	1E-15	1E-15	++☐ Structure015(1)	7.7	1.3	0.0059
++☐ Structure016(1)	0.0	1E-15	1E-15	++☐ Structure016(1)	3.4	1.17	0.00484
++☐ Structure017(1)	0.0	1.42	0.00714	++☐ Structure017(1)	11.3	2.31	0.0187
++☐ Structure018(1)	0.0	0.889	0.00278	++☐ Structure018(1)	0.0	1E-15	1E-15
++☐ Structure019(1)	0.0	1E-15	1E-15	++☐ Structure019(1)	12.7	2.78	0.0272
++☐ Structure020(1)	0.0	1E-15	1E-15	++☐ Structure020(1)	0.0	1E-15	1E-15
++☐ Structure021(1)	0.0	0.363	0.000465	++☐ Structure021(1)	8.8	1.58	0.00876
++☐ Structure022(1)	0.0	1E-15	1E-15	++☐ Structure022(1)	0.0	1E-15	1E-15
++☐ Structure023(1)	0.0	1E-15	1E-15	++☐ Structure023(1)	0.0	1E-15	1E-15
++☐ Structure024(1)	0.0	2.06	0.0149	++☐ Structure024(1)	0.0	1E-15	1E-15
++☐ Structure025(1)	0.0	1E-15	1E-15	++☐ Structure025(1)	0.2	12.3	0.52

Figure 8. Tabular results of an ammonium nitrate explosion equivalent to 907.2 metric tons of trinitrotoluene.

Table 6. Damage classification and damage level.

Level	Building Damage
Slight	Superficially damaged. No permanent deformation in the primary and secondary structural members, or non-structural elements.
Moderate	Damage – repairable. Minor deformations in the non-structural elements and secondary structural members, and no permanent deformation in the primary structural members.
Severe	Damaged – unrepairable. Major deformation in non-structural elements and secondary structural members and minor deformation of primary structural members, but progressive collapse is unlikely.

tons of TNT. The building damage resulting from the ExDAM 3D explosion simulation is shown in Figure 7. Figure 8 shows the numerical results of the damage to buildings caused by the explosion. The 907.2 metric tons TNT-equivalent explosion affected 1598 out of 4708 buildings, with an estimated building damage of 58423084944 KRW (approximately 47,600,000 US dollars). The damage costs are listed in Table 8.

Therefore, the explosions of 500.5 or 2160 metric tons of ammonium nitrate resulted in damage of approximately 44616934076 KRW (~36,000,000 US dollars) or 58423084944 KRW (~47,600,000 US dollars), respectively.

Table 7. Cost of damage caused by the explosion of ammonium nitrate equivalent to 210.21 metric tons of trinitrotoluene.

Building Number	Usage Code	Material Code	Total Area (m^2)	Standard Unit Price (KRW)	Damage (%)	Cost (KRW)
Structure001	U-7	M-1	51.84	1 640 448	8.5	7 228 470
Structure002	U-7	M-9	87.87	1 640 448	2.1	3 027 069
Structure013	U-7	M-4	62.37	1 640 448	0.5	511 574
Structure015	U-7	M-2	68.6	1 640 448	4.9	5 514 202
Structure016	U-7	M-4	57.39	1 640 448	1.5	1 412 180
Structure017	U-7	M-2	40.8	1 640 448	8.1	5 421 353
••••	••••	••••	••••	••••	••••	••••
Structure4688	U-19	M-9	349.94	1 453 844	0.3	1 526 275
Structure4689	U-19	M-9	242	1 453 844	0.4	1 407 321
Structure4692	U-7	M-9	90.6	1 640 448	2.3	3 418 366
Structure4700	U-7	M-2	26	1 640 448	9.9	4 222 513
Structure4704	U-7	M-9	148.75	1 640 448	1.2	2 928 200
Structure4708	U-7	M-2	204.04	1 640 448	5.3	17 740 002
Total Cost (KRW)	**44 616 934 076**					

Table 8. Costs of damage caused by the explosion of ammonium nitrate equivalent to 907.2 metric tons of trinitrotoluene.

Building Number	Usage Code	Material Code	Total Area (m^2)	Standard Unit Price (KRW)	Damage (%)	Cost (KRW)
Structure001	U-7	M-1	51.84	1 640 448	13.9	11 820 675
Structure002	U-7	M-9	87.87	1 640 448	4.9	7 063 162
Structure011	U-3	M-5	1473.07	1 133 590	0.1	1 669 857
Structure013	U-7	M-4	62.37	1 640 448	1.2	1 227 777
Structure015	U-7	M-2	68.6	1 640 448	7.7	8 665 174
Structure016	U-7	M-4	57.39	1 640 448	3.4	3 200 941
Structure017	U-7	M-2	40.8	1 640 448	11.3	7 563 121
Structure019	U-7	M-2	112.18	1 640 448	12.7	23 371 233
Structure021	U-7	M-2	74.84	1 640 448	8.8	10 803 859
••••	••••	••••	••••	••••	••••	••••
Structure4686	U-22	M-8	13 875.03	989 456	0.2	27 457 463
Structure4687	U-3	M-5	1956.17	1 172 500	2.4	55 046 624
Structure4688	U-19	M-9	349.94	1 453 844	0.7	3 561 307
Structure4689	U-19	M-9	242	1 453 844	0.8	2 814 642
Structure4692	U-7	M-9	90.6	1 640 448	5.4	8 025 728
Structure4700	U-7	M-2	26	1 640 448	15.5	6 611 005
Structure4704	U-7	M-9	148.75	1 640 448	3	7 320 499
Structure4708	U-7	M-2	204.04	1 640 448	12.2	40 835 475
Total Cost (KRW)	**58 423 084 944**					

7. Conclusions

Currently, in addition to ammonium nitrate, a variety of explosives are stored and distributed at the Busan ports, which could explode and cause fatal damage. We are obligated to minimize damage through the establishment of safety plans for prevention and preparation, as long as there is the possibility of an explosion accident, and we must raise awareness of explosive safety management.

This study presented a method for calculating the amount of economic damage due to an explosion accident to evaluate the risk of a large-scale explosion in advance. Using 3D explosion simulation and GIS spatial information, the physical characteristics of the explosion were considered by considering the building materials, shielding effects, and building information that was not applied in previous studies. The scale of the potential explosion was measured, and the damage level of each building exposed to the explosion was calculated. This was converted into the amount of economic damage based on the building's use, and three studies were conducted to raise awareness about explosive safety management and provide a basis for decision-making. The studies were performed in the following order: scenario configuration, hazard and vulnerability analysis using GIS spatial information, 3D expansion simulation, and economic risk assessment. The results derived from conducting the research at each stage are as follows.

1. The scenario was composed of two reliable explosion accident scenarios based on the actual cargo volume and storage volume of ammonium nitrate at Busan Port, which is the cause of many large-scale explosions worldwide. The TNT equivalent conversion for ammonium nitrate was performed for realistic damage prediction, and data from the US Department of Defense and the Korea Occupational Safety and Health Agency were used.
2. Hazard and vulnerability analyses were performed using GIS spatial information and explosion simulations. The government-constructed building spatial information was used to analyze 4708 buildings within a 3 km radius of the explosion area, allowing for a wide range of hazard areas and impact analysis. The explosion impact was determined, and a vulnerability analysis was performed by considering the building material, height, and location information for each building.
3. The research results were derived for economic risk assessment by multiplying the building damage level, which is the result value

derived from the 3D explosion simulation, by the unit cost of new construction and the total floor area of the building, based on the use suggested by the Korea Real Estate.

Port managers and business operators can apply location information, storage volume, and characteristics of dangerous substances stored in the workplace to the presented risk assessment method to recognize the risk of dangerous substances and suggest effective improvement measures. As this study was based on a scenario in risk assessment, a deterministic methodology was used. Because chemical accidents are caused by technical accidents due to human error, it is difficult to determine the results of the reproduction cycle and frequency analysis. In the field of industrial safety, the frequency of occurrence is calculated based on the design of operating facilities; however, it is difficult to analyze the frequency of outdoor explosion accidents at ports. In the future, a big data accident case or new frequency analysis method will be required for risk assessment based on probability. To advance this study, it will be necessary to investigate economic risk assessment methods that consider human and social vulnerabilities, as well as dynamic factors, rather than simply calculating economic damage based on building damage levels. For strategic planning, technology that can evaluate outdoor effects beyond modeling and simulation of hazardous-chemical leakage and chemical explosion accidents should be combined with GIS technology to continue to attempt vulnerability and risk assessments in terms of disaster management. As this study presents a new method of risk evaluation in the field of chemical accidents, we expect that the findings will help in decision making for realizing a safe society.

Declarations

Author contribution statement

Jae-Joon Lee : Conceived and designed the experiments; Analyzed and interpreted the data; Contributed reagents, materials, analysis tools or data; Wrote the paper. Review & editing

Woo Song Jeong: Performed the experiments; Wrote the paper; Contributed analysis tools or data; Review & editing.

Tae-Yuun Ham : Performed the experiments; Analyzed and interpreted the data; Wrote the paper; Contributed analysis tools and data

Funding statement

This work was supported by the National Research Foundation of Korea(NRF) under Grant [2021R1C1C2010999], This research was supported by a grant (2019-MOIS33-005) of Lower-level and Core Disaster-Safety Technology Development Program funded by the Ministry of Interior and Safety (MOIS, Korea).

Data availability statement

Data will be made available on request.

Declaration of interest's statement

The authors declare no competing interests.

Additional information

No additional information is available for this paper.

References

[1] X. Baraza, A. Pey, J. Giménez, The self-sustaining decomposition of ammonium nitrate fertiliser: case study, Escombreras valley, Spain, J. Hazard Mater. 387 (2020), 121674.
[2] J.Y. Choi, J.Y. Choi, A Study on the Response Capability of the Enhancements through the Analysis of Tianjin Explosion Accident in China, 2016.
[3] S. Kwon, H.Y. Kim, Analysis of Explosion Energy Related to the Cause of Tianjin Explosion Accident in China vol. 34, 2016, pp. 1–10.
[4] G. Yu, Y. Wang, L. Zheng, J. Huang, J. Li, L. Gong, et al., Comprehensive study on the catastrophic explosion of ammonium nitrate stored in the warehouse of Beirut port, Process Saf. Environ. Protect. 152 (2021) 201–219.
[5] S. Sivaraman, S. Varadharajan, Journal of Loss Prevention in the Process Industries Investigative consequence analysis : a case study research of beirut explosion accident, J. Loss Prev. Process. Ind. 69 (2021), 104387.
[6] W. Pittman, Z. Han, B. Harding, C. Rosas, J. Jiang, A. Pineda, et al., Lessons to be learned from an analysis of ammonium nitrate disasters in the last 100 years, J. Hazard Mater. 280 (2014) 472–477.
[7] D.M. Laboureur, Z. Han, B.Z. Harding, A. Pineda, W.C. Pittman, C. Rosas, et al., Case study and lessons learned from the ammonium nitrate explosion at the West Fertilizer facility, J. Hazard Mater. 308 (2016) 164–172.
[8] S. Zhang, H. Ma, X. Huang, S. Peng, Numerical simulation on methane-hydrogen explosion in gas compartment in utility tunnel, Process Saf. Environ. Protect. 140 (2020) 100–110.
[9] S. Wang, Z. Li, Q. Fang, H. Yan, Y. Liu, Numerical simulation of overpressure loads generated by gas explosions in utility tunnels, Process Saf. Environ. Protect. 161 (2022) 100–117.
[10] Q. Xu, K. Xu, Safety assessment of sand casting explosion accidents through on-site testing and numerical simulation of the temperature variation in sand molds to protect employee health, Process Saf. Environ. Protect. 159 (2022) 452–463.
[11] F. Ustolin, I.C. Tolias, S.G. Giannissi, A.G. Venetsanos, N. Paltrinieri, A CFD analysis of liquefied gas vessel explosions, Process Saf. Environ. Protect. 159 (2022) 61–75.
[12] L. Zhang, H. Wang, C. Chen, P. Wang, L. Xu, Experimental study to assess the explosion hazard of CH4/coal dust mixtures induced by high-temperature source surface, Process Saf. Environ. Protect. 154 (2021) 60–71.
[13] J.W. Luo, Q.H. Wang, Y.H. Chung, V. Volli, C.M. Shu, Y.C. Cheng, Hazard evaluation, explosion risk, and thermal behaviour of magnesium- aluminium alloys during the polishing process by using a 20-L apparatus, MIEA, and TGA, Process Saf. Environ. Protect. 153 (2021) 268–277.
[14] M. Li, H. Wang, D. Wang, Z. Shao, S. He, Risk assessment of gas explosion in coal mines based on fuzzy AHP and bayesian network, Process Saf. Environ. Protect. 135 (2020) 207–218.
[15] Q. Li, S. Zhou, Z. Wang, Quantitative risk assessment of explosion rescue by integrating CFD modeling with GRNN, Process Saf. Environ. Protect. 154 (2021) 291–305.
[16] S. Dan, C.J. Lee, J. Park, D. Shin, E.S. Yoon, Quantitative risk analysis of fire and explosion on the top-side LNG-liquefaction process of LNG-FPSO, Process Saf. Environ. Protect. 92 (2014) 430–441.
[17] R. Jena, B. Pradhan, S.P. Naik, A.M. Alamri, Earthquake risk assessment in NE India using deep learning and geospatial analysis, Geosci. Front. 12 (2021), 101110.
[18] R. Jena, B. Pradhan, G. Beydoun, A.M. Alamri, Nizamuddin Ardiansyah, et al., Earthquake hazard and risk assessment using machine learning approaches at Palu, Indonesia, Sci. Total Environ. 749 (2020), 141582.
[19] S. Tesfamariam, K. Goda, Risk assessment of CLT-RC hybrid building : consideration of earthquake types and aftershocks for Vancouver , British Columbia, Soil Dynam. Earthq. Eng. 156 (2022), 107240.
[20] K. Goda, V. Novelli, R. De Risi, P. Kloukinas, N. Giordano, J. Macdonald, et al., Scenario-based earthquake risk assessment for central-southern Malawi: the case of the Bilila-Mtakataka Fault, Int. J. Disaster Risk Reduc. 67 (2022), 102655.
[21] G. Antonioni, G. Spadoni, V. Cozzani, A methodology for the quantitative risk assessment of major accidents triggered by seismic events, J. Hazard Mater. 147 (2007) 48–59.
[22] K. Zhang, M.H. Shalehy, G.T. Ezaz, A. Chakraborty, K.M. Mohib, L. Liu, An integrated flood risk assessment approach based on coupled hydrological-hydraulic modeling and bottom-up hazard vulnerability analysis, Environ. Model. Software 148 (2022), 105279.
[23] K. Schröter, M. Barendrecht, M. Bertola, A. Ciullo, R.T. da Costa, L. Cumiskey, et al., Large-scale flood risk assessment and management: prospects of a systems approach, Water Secur. 14 (2021), 100109.
[24] G. Zhi, Z. Liao, W. Tian, J. Wu, Urban flood risk assessment and analysis with a 3D visualization method coupling the PP-PSO algorithm and building data, J. Environ. Manag. 268 (2020), 110521.
[25] H.M. Lyu, W.J. Sun, S.L. Shen, A. Arulrajah, Flood risk assessment in metro systems of mega-cities using a GIS-based modeling approach, Sci. Total Environ. 626 (2018) 1012–1025.
[26] United States Environmental Protection Agency, Explosion hazard from ammonium nitrate, in: US EPA Arch Doc, vol. 10, 1997, pp. 1–6.
[27] H.Q. Cao, Q.L. Duan, H. Chai, X.X. Li, J.H. Sun, Experimental study of the effect of typical halides on pyrolysis of ammonium nitrate using model reconstruction, J. Hazard Mater. 384 (2020), 121297.
[28] J. Sun, Z. Sun, Q. Wang, H. Ding, T. Wang, C. Jiang, Catalytic effects of inorganic acids on the decomposition of ammonium nitrate, J. Hazard Mater. 127 (2005) 204–210.
[29] C. Oommen, S.R. Jain, Ammonium nitrate: a promising rocket propellant oxidizer, J. Hazard Mater. 67 (1999) 253–281.
[30] M.V. Shubov, Drone launched short range rockets, Aerospace 7 (2020).
[31] V. Babrauskas, Explosions of ammonium nitrate fertilizer in storage or transportation are preventable accidents, J. Hazard Mater. 304 (2016) 134–149.
[32] H.J. De Lange, S. Sala, M. Vighi, J.H. Faber, Ecological vulnerability in risk assessment - a review and perspectives, Sci. Total Environ. 408 (2010) 3871–3879.
[33] A. Preciado, A. Ramirez-Gaytan, R.A. Salido-Ruiz, J.L. Caro-Becerra, R. Lujan-Godinez, Earthquake risk assessment methods of unreinforced masonry structures: hazard and vulnerability, Earthq Struct 9 (2015) 719–733.

[34] M. Masood, K. Takeuchi, Assessment of flood hazard, vulnerability and risk of mid-eastern Dhaka using DEM and 1D hydrodynamic model, Nat. Hazards 61 (2012) 757–770.
[35] H. Ha, Q.D. Bui, H.D. Nguyen, B.T. Pham, T.D. Lai, C. Luu, A practical approach to flood hazard, vulnerability, and risk assessing and mapping for Quang Binh province, Vietnam, Environ. Dev. Sustain. (2022).
[36] C.J. Van Westen, Remote sensing and GIS for natural hazards assessment and disaster risk management, Treatise Geomorphol. 3 (2013) 259–298.
[37] C. Van Westen, Geo-Information tools for landslide risk assessment: an overview of recent developments, Landslides Eval. Stab. Terrain Eval. Stabil., Set 2 (2004) 39–56.
[38] A.S. Soomro, A. Qadeer, K. Rajput, S.H. Solangi, GIS-based fast moving landslide risk analysis model using qualitative approach: a case study of Balakot, Pakistan, Risk Anal. 30 (2011) 307–318.
[39] C.J. van Westen, van Asch TWJ, R. Soeters, Landslide hazard and risk zonation - why is it still so difficult? Bull. Eng. Geol. Environ. 65 (2006) 167–184.
[40] R.K. Wharton, S.A. Formby, R. Merrifield, Airblast TNT equivalence for a range of commercial blasting explosives, J. Hazard Mater. 79 (2000) 31–39.
[41] E.D. Esparza, Blast measurements and equivalency for spherical charges at small scaled distances, Int. J. Impact Eng. 4 (1986) 23–40.
[42] P.W. Cooper, Comments on TNT equivalence, in: 20th Int Pyrotech Semin, 1994, pp. 215–226.
[43] I. Sochet, Blast Effects of External Explosions to Cite This Version:HAL Id:Hal-00629253, 2011.
[44] A.B. Alias, K. Halim, K. Hamid, M. Bani, U. Kristen, D. Wacana, Analysis the Effect of Explosion Efficiency in the TNT Equivalent Blast Explosion Model, Icgsce, 2015.
[45] T. Ngo, R. Lumantarna, A. Whittaker, P. Mendis, Quantification of the blast-loading parameters of large-scale explosions, J. Struct. Eng. 141 (2015), 04015009.
[46] H.J. Pasman, C. Fouchier, S. Park, N. Quddus, D. Laboureur, Beirut ammonium nitrate explosion: are not we really learning anything? Process Saf. Prog. 39 (2020).
[47] R. Hutchison, P. Skinner, Ammonium Nitrate in Ports – Storage and Transportation, 2007, pp. 1–5.
[48] U.S. Army, Explosives and Demolitions Manual, 2007.
[49] T. Consultants, BREEZE ExDAM 8.5 User Guide, 2014.
[50] Glasstone S, Dolan PJ. The Effects of Nuclear Weapons. third ed. n.d.
[51] J.J. Lee, H.S. Yun, Y.J. Cho, J.H. Park, Empirical analysis of a steam explosion in a slag yard based on a field investigation and 3D explosion damage simulation, Process Saf. Environ. Protect. 136 (2020) 126–135.
[52] Defense Intelligence Agency, Mathematical Background and Programming Aids for the Physical Vulnerability System for Nuclear Weapons. DI-SSU-27-4, 1974.
[53] Code L. Study on the Impact Assessment of Explosion Damage n.d.
[54] H. Rouse, Elementary Mechanics of Fluids/by Hunter Rouse, 1978.
[55] C. Oswald, E. Conrath, A Computer Program for Explosive Damage Assessment of Conventional Buildings, Proc Twenty-Sixth DoD Explos Saf Semin, 1994.
[56] M. Hyun, Application of multi-dimensional flood damage analysis in urban area, J. Korea Water Resour. Assoc. 50 (2017) 397–405.
[57] K. Zhou, L. Xiao, Y. Lin, D. Yuan, J. Wang, A statistical analysis of hazardous chemical fatalities (HCFs) in China between 2015 and 2021, Sustainability 14 (2022) 2435.
[58] R.A. Freeman, CCPS guidelines for chemical process quantitative risk analysis, Plant/Operations Prog 9 (1990) 231–235.
[59] K. Rajeev, S. Soman, V.R. Renjith, P. George, Human vulnerability mapping of chemical accidents in major industrial units in Kerala, India for better disaster mitigation, Int. J. Disaster Risk Reduc. 39 (2019), 101247.
[60] T.H. Miller, T. Stevens, C.R. Rath, C.M. Tenney, M.K. Kinnan, M. Pepple, Chemical Incident Economic Impact Analysis Methodology, 2013.